UNIVERSITÀ DEGLI STUDI DI TRENTO
Facoltà di Scienze Matematiche, Fisiche e Naturali

Corso di Laurea triennale in Fisica

Elaborato finale

Josephson Effect and Selected Applications: an Example of Quantum Effects in Macroscopic Systems

Relatore:
Prof. Giovanni Andrea Prodi

Laureando:
Fabio Zanini

Anno Accademico 2007 - 2008

Contents

Introduction

The Josephson effect is a classic topic in superconductivity. It was predicted by B. D. Josephson in 1962, when he was 22 years old. It appears in the so-called Josephson junction. This is a structure formed by two superconductors close to each other, but separated with an oxide layer. It is in fact not a single effect; it is composed by several phenomena that are explained through the same theoretical framework, i.e. the Josephson theory.

There are many reasons for which I chose this topic for my dissertation. Among them, the most relevant are the following:

- it entangles many branches of physics, like quantum mechanics, condensed matter, electronics, atomic gases;
- the Josephson theory is, in the version I have used, quite simple, but very general;
- it is the source of several important applications in various fields of human activity, from medicine to computer technology;
- it recently regained the interest of basic research scientists, because of its analogs in superfluids and trapped atomic gases;
- I had the chance to go into the laboratory and observe it personally.

The structure of the thesis is the following. There are three main chapters. In the first one, the physical foundations of the Josephson effect are investigated. A short overview of quantum mechanics and classical mechanics is presented, and some important differences are stressed. The issue of quantum decoherence is addressed. Appearance of quantum effects in macroscopic bodies is discussed, followed by a brief overview of superconductivity.

In the second chapter, the theory of the Josephson effect is developed. For the sake of simplicity and generality, the approach of Feynman is followed[1]. A model of Josephson junctions is introduced, and its characteristics and limits are discussed. In the last section, some experimental data, collected during last spring term by some colleagues and me, are shown.

The third chapter is devoted to applications and recent research progresses. Historically relevant applications are reviewed: SQUID, voltage standard, and computer technology. Analogs of the Josephson effect in other system than superconductors occupy the last part of the thesis. Atomic Bose gases have been given special attention.

Aknowledgements

I want to thank my supervisor, Prof. Giovanni Andrea Prodi, for the corrections and useful advice that he gave me, and for his good mood.

Then I thank Prof. D. Kölle at Universität Tübingen for his explanations about the Josephson effect, and for allowing me to observe the phenomenon. I also thank my colleagues Teresa Selistrovski, Georg Kurij, and Alexander Opitz, who were responsible for the good quality of the experimental data. Teresa was so kind to write the experimental report, and to send it to me. I want to show my appreciation to Dott. Ricci, the supervisor of the "Doppia Laurea" project, for his logistic, scientific and moral help before and during the writing of this thesis. I am also thankful to Prof. Dalfovo and Prof. Stringari, who were so kind to suggest me some references on Bose Einstein Condensation.

Finally, I would like to cite Donald Knuth, and all other computer programmers who wrote the free applications that I used for this work.

There were obviously many other people who helped me in some way, and whom I thank very much; they already know it.

Chapter 1

Foundational remarks

The Josephson effect is based on the behaviour of a quantum parameter called phase. In this chapter we briefly investigate the physical and mathematical foundations of the effect. In the first section, the main characteristics of quantum mechanics are recalled. In the second section, we explain the reason, for which classical mechanics is inapplicable. The third section deals with statistics. It touches on the topic of quantum information, and states some intuitive general conditions for the appearance of quantum macroscopic effects. Finally, the last section is a short overview of (low-temperature, type I) superconductivity.

1.1 Microscopic theory of matter: QM

The simplest self-consistent theory of matter is nonrelativistic quantum mechanics (NRQM). It is well known that it does not take into account all observed natural phenomena, *inter aliis* spontaneous emission and finite speed of light. Substantial improvements have been achieved through more modern approaches, such as Relativistic Quantum Mechanics and Quantum Field Theory. Nevertheless, NRQM is still by far the preferred theoretical framework of low-energy condensed-matter physics, mainly because of its relative mathematical simplicity and its not-so-involved physical interpretation.

1.1.1 States and observables

In the context of NRQM, a particle $\mathbf{P}$ is described through a vector $|\Psi_{\mathbf{P}}>$ of an appropriate complex-valued Hilbert space $\mathcal{H}$. If a particular basis of $\mathcal{H}$ is specified, the whole description of $\mathbf{P}$ is in the time-dependent components $c_{\mathbf{k}}$ of its vector respect to this basis. The number of these components can be, depending on the experimental setup, finite or infinite. Moreover, the components can be discrete or continuous.

Quantum Mechanics is assumed to be a *complete* theory of matter, rather than a partial self-consistent approach. This means: the knowledge of all (possibly infinite) components of $|\Psi_{\mathbf{P}}>$ contains the whole experimentally obtainable information on $\mathbf{P}$. It is impossible to build or even imagine an experiment, in which more information can be extracted from a system, than that contained in $|\Psi_{\mathbf{P}}>$. In this sense QM admits no "hidden variables".

The completeness hypothesis is surely false for the nonrelativistic version of the theory which is used here, since it entirely ignores a feature of elementary particles, i.e. *spin*. Fortunately, the spin σ can be approximately incorporated into NRQM through simple tensor product of its Hilbert space $\mathcal{H}_\sigma$ with the space $\mathcal{H}_k$ of all other properties k:

$$\mathcal{H} = \mathcal{H}_k \otimes \mathcal{H}_\sigma \qquad\qquad |\Psi_{\mathbf{P}}>= |k_{\mathbf{P}}> \otimes |\sigma_{\mathbf{P}}> \tag{1.1}$$

On the one hand this non-native addition of the spin limits the predictive power of the theory. For instance, it excludes proper fine and hyperfine corrections to the hydrogen spectrum. On the other hand, it allows one to study a problem at first without the spin complexity and to include it at a later stage, when a certain physical intuition of the solution has already been developed. Furthermore, the results of the simplified theory (i.e. without spin) are often precise enough to agree with experimental data. In the following we will restrict our description to this simplified NRQM. Its macroscopic counterpart 1.4.5 explains sufficiently well the phenomena involved in the Josephson effect[1].

Physical properties of $\mathbf{P}$ can be extracted from $|\Psi_{\mathbf{P}}>$ through *observables*, linear functions from $\mathcal{H}$ to itself which have mathematical features necessary to assure the self-concistency of the theory. The connection with experiments is the following[2]. When we measure a certain physical quantity O, we choose a basis of $\mathcal{H}$ formed by eigenvectors of the observable $\mathbf{O}$ describing O. Every single experimental result is just one of the eigenvalues of $\mathbf{O}$. If we perform many experiments in exactly the same conditions, we do not in general find always the same result, but rather all possible eigenvalues, with a fixed probability distribution. The mean value corresponds to the *expectation value* of $\mathbf{O}$, defined by:

$$<\mathbf{O}>_{\Psi_{\mathbf{P}}} := <\Psi_{\mathbf{P}}|\mathbf{O}|\Psi_{\mathbf{P}}> \tag{1.2}$$

where the bra-ket notation has the meaning of a scalar product.

1.1.2 Spectral decomposition, stationary states and wavefunction

The list of all possible eigenvalues of an observable is called *spectrum*. As a consequence of the famous *spectral theorem*, it is possible to form a basis

[1] The original version of the Josephson theory does make use of the spin[2].

[2] For a introduction to the mathematics of QM, see e.g. [3] (in italian).

of $\mathcal{H}$ made by eigenvectors of an observable $\mathbf{O}$. This procedure is called *spectral decomposition*. The general form of the state of $\mathbf{P}$ is:

$$|\Psi_{\mathbf{P}}>=\sum_{\mathbf{k}} c_{\mathbf{k}}\,|\mathbf{k_O}> \quad \text{or} \quad |\Psi_{\mathbf{P}}>=\int_{\mathbf{k}} \mathrm{d}\mathbf{k}\, c_{\mathbf{k}}\,|\mathbf{k_O}> \tag{1.3}$$

depending of the discreteness or continuousness of $\mathbf{k}$, where $|\mathbf{k_O}>$ are eigenvectors of $\mathbf{O}$.

An interesting decomposition is that of the hamiltonian. An eigenvector of $\mathbf{H}$ is called *stationary state*. Its eigenvalue $E_{\mathbf{k}}$ is the energy of that state. If the hamiltonian is time-indipendent, as it is in most cases in condensed-matter experiments, the energies are also time-indipendent. Being the evolution equation the following:

$$i\hbar\frac{\partial}{\partial t}|\Psi_{\mathbf{P}}>=\mathbf{H}|\Psi_{\mathbf{P}}> \qquad \textbf{Schrödinger equation} \tag{1.4}$$

in which $\mathbf{H}$ is the hamiltonian observable describing the interaction of $\mathbf{P}$ with the world, it results for a stationary state:

$$|\mathbf{k_H}>(t)=e^{-iE_{\mathbf{k}}t/\hbar}|\mathbf{k_H}>(0)$$

Stationary states are of primary importance, since they allow to decouple time in the evolution equation; the $c_{\mathbf{k}}$ are time-indipendent. In particular, a particle in a stationary state will remain there forever.

Now, let us choose as observable the position operator $\mathbf{x}$. We get a continuous decomposition:

$$|\Psi_{\mathbf{P}}>=\int_{\mathbf{x}} \mathrm{d}\mathbf{x}\, c_{\mathbf{x}}\,|\mathbf{x}>$$

The coefficients constitute in fact a continuous function of $\mathbf{x}$, which is usually written $\psi(x,t) := c_{\mathbf{x}}$ and called *wavefunction*. Its squared norm $|\psi(x,t)|^2$ gives the probability density that the particle is measured at the position $\mathbf{x}$ at time t. A *probability current*, which is an estimator of the movement of $\mathbf{P}$, can be defined:

$$\mathbf{J}=\frac{i\hbar}{2m}\left[(\psi\nabla\psi^*-\psi^*\nabla\psi)-\frac{q}{m}\mathbf{A}|\Psi(x,t)|^2\right] \tag{1.5}$$

The wavefunction takes complex values; it has a definite *phase* for every ($\mathbf{x}$,t). It can be easily shown that the *total phase* of Ψ can be shifted by an arbitrary amount without changing the physics of $\mathbf{P}$. The only important point is the pairwise *phase difference* between two components $c_{\mathbf{k}}$. This difference enters directly the Josephson theory, as we will see later.

1.1.3 Many-particle QM

We have so far dealt with a single particle. The extension to the many-particle description is well beyond the scope of this thesis, however some remarks are mandatory:

- many-particle systems are also described by states and operators;
- stationary states exist also in many-particle QM and have the same role;
- the dimension of $\mathcal{H}$ is significantly increased.

The last observation can alternatively be cast in the following form: the number of complex parameters[3] necessary to describe completely a many-particle system is *extremely* high. Among other things, the phase of every parameter has to be determined to specify the state of the system.

Because of this reason, a pure quantum mechanical approach to macroscopic bodies would be a formidable, probably impossible task. One has to rely either on statistical methods (see section 1.3), or on macroscopically phenomenological theories like Classical Mechanics (see next section).

1.2 Macroscopic theory of matter: CM

In opposition to QM, the simplest theory able to handle macroscopical systems is Nonrelativistic Classical Mechanics (NRCM). As for NRQM, it does not explain vacuum-connected or extreme relativistic phenomena, still it is well-suited for most ordinary situations.

1.2.1 Real tensors description

There are many different versions of NRCM, the most useful for our purposes is the Hamiltonian formulation. The properties of a particle **P** are given by real tensor fields on the phase space, which correspond in NRMQ both to states and operators. Position and momentum are taken as fundamental variables, on which all other tensors depend.

Classical Mechanics is in no way a complete theory. From the discovery of the atomic nature of matter on, physicists are well conscious that NRCM is no more than a large-scale approximation of microscopic theories like NRQM. Thus a particle **P** can have, besides all tensorially described features, other "hidden" properties which are smoothed out in the large-scale limit.

[3]For instance, (complex) coefficients or (complex-valued) wave-like functions.

1.2.2 Many-subparticle CM

From a foundational point of view, the very concept of "particle" is quite arbitrary in CM, because of its interisically macroscopic nature. In a Galileo-like perspective, we could assume that a small, non-rotating ball is a good physical realization of a particle. At the same time, we are aware that even the smallest macroscopical ball is internally composed by a great number of subparticles. The problem is resolved by imposing *constraints* on the subparticles, in order to reduce drastically the number of variables of the system. For instance, the famous rigid body condition limits the number of positional coordinates to 6 (or less), whatever the initial number of coordinates.

The possibility of describing a macroscopic body through classical mechanics is a huge simplification, if compared to a quantum mechanical description. Our problem is the following: classical mechanics does not predict any Josephson effect at all. Since in NRCM all quantities are real, the very concept of phase becomes meaningless. We have to find an alternate path to build a theory for the Josephson effect. As explained in the previous section 1.1.3, this has to pass through statistics.

1.3 Statistical properties and decoherence

Now we have to front the following puzzling issue: why can we successfully describe macroscopic bodies with a simple theory based on few variables like NRCM? A macroscopic body contains a great number of quantum particles, nonetheless we can safely ignore all single-particle variables and study only properties of the whole body. Where are all other "hidden variables" eventually hidden?

The central point is that in almost all macroscopic experiments we are dealing with statistical behaviours and average quantities. The microscopical features of a body can emerge in three different ways from the averaging process. Firstly there are some properties with nonvanishing mean and whose effects can be included in a constraint-featured macroscopic theory. For example it is the case of positions and velocities of rigid bodies. Secondly it can come up that some microscopical features show evident macroscopical effects, but they can not be easily included into macroscopic theories because of practical difficulties in calculations. In this case, for example by glass theories or quantum chemistry, efforts are put in phenomenological and numerical calculations. Increasingly better approximated theories are developed. Finally, some microscopical variables are just smoothed out by many-particle statistics and do never - or almost never - show any significant effect on macroscopic scale experiments. The last situation refers also to the phase differences among all quantum particles of a body. This loss of information is generally called *decoherence*.

1.3.1 The origin of decoherence

The origin of decoherence lays in the very hearth of NRQM, in the concept of stationary state. We have already said that knowing the state of a quantum system **S** is equivalent to knowing all of **S**. For a stationary state, a knowledge of the state $|\mathbf{k_H}>$ of **S** includes the energy $E_\mathbf{k}$ of the state.

If the allowed energies of the system were pairwise well separated, this requirement could be fulfilled. In fact, this is exactly what happens in one-particle experiments. The problem with macroscopic bodies is that they show an "extremely high density of levels in the energy eigenvalue spectrum", as Landau points out in [4, 14]. Two dramatic consequences follow from this fact.

On the one hand, a macroscopic system **S** feels small, unpredictable interactions with the environment. Because of the high density of states of the body, these forces continuously change the state of **S**, in a random way. The state description is therefore unusable.

On the other hand, every process that brings a system **S** into a stationary state $|\mathbf{k_H}>$ takes some time to act. But in the quantum world the energy-time uncertainty principle holds. If the energy difference between $|\mathbf{k_H}>$ and the many neighbour stationary states is very small, the minimal time of the process is very large. For short times we can only determine a certain "state range". The whole state description collapses again.

The main result of the preceding analysis is that the exact complex-valued state description of matter is inapplicable to systems, which interact with their environment. All practical macroscopic bodies enter this category, with few exceptions which we present in section 1.3.3. Therefore another approach is used, a statistical and more phenomenological one.

1.3.2 Decoherence as a fundamental working hypothesis

The central property of quantum statistical mechanics to eliminate the phase is clearly explained by Huang[5, 173]. A *Postulate of random phases* is introduced at the beginning of the theory. It states that the coefficients of the spectral decomposition of a macroscopic state onto a basis made of stationary states have random phases. In this way, we accept as a principle of Nature to lose any information about the phase.

This fundamental assumption is justified by the fact that it leads to results in agreement with experiments. In other words, it is a phenomenological hypothesis which does not derive from NRQM.

The solution of the decoherence problem through this *ad hoc* assumption has been judged unsatisfactory by some scientists. Modern studies on *entanglement*, i.e. general quantum phase interference, try to shed some light onto this topic. However, state-of-the-art theories and experiments are still quite at a draft level, and the phenomenon is not completely understood.

In the following, we accept the postulate of random phases "as is", without further investigations.

1.3.3 Coherent macroscopic states

It can be shown that the preceding discussion "is inapplicable to the initial part of the energy spectrum; the separations between the first few energy levels of a macroscopic body may even be independent of the size of the body[4, 15,footnote]". Generally speaking, it could be possible to find a macroscopic body showing quantum effects if the following two conditions are fulfilled:

1. the body occupies the first few energy levels;
2. the energy gaps ΔE_{ij} among these levels are indipendent of the size of the body and bigger than the mean thermal energy $\Delta E_{ij} \gtrsim kT$;

Both conditions have good chances to be satisfied if the temperature is very low. This is exactly what happens in superconductivity. In this case the decoherence does not arise and it is quite intuitive that the system could remain in a precise quantum state for a relatively long time. Therefore it makes sense to speak of a *quantum state of the macroscopic system* or more briefly *macroscopic state*.

Strictly speaking, the above conditions are not necessary for the appearance of quantum macroscopic effects. For instance, semiconductors are also based on a quantum effect (energy bands) in large-scale systems.

1.4 Superconductivity

Superconductivity is a phenomenon of low-temperature solid-state physics. It consists mainly of two experimental evindences:

- in a supercondicting material, an electric current can flow without any resistance;
- a superconducting piece of matter is perfectly diamagnetic apart from a thin surface layer.

Although the microscopic theory is quite involved and far from being complete (see e.g. [6, 23-94]), the key mechanism is rather well understood.

1.4.1 Energy gap

The single-electron density of states in a superconductor, i.e. a solid block of matter which shows the superconducting properties, is not everywhere very high, as in a "normal" macroscopic body.

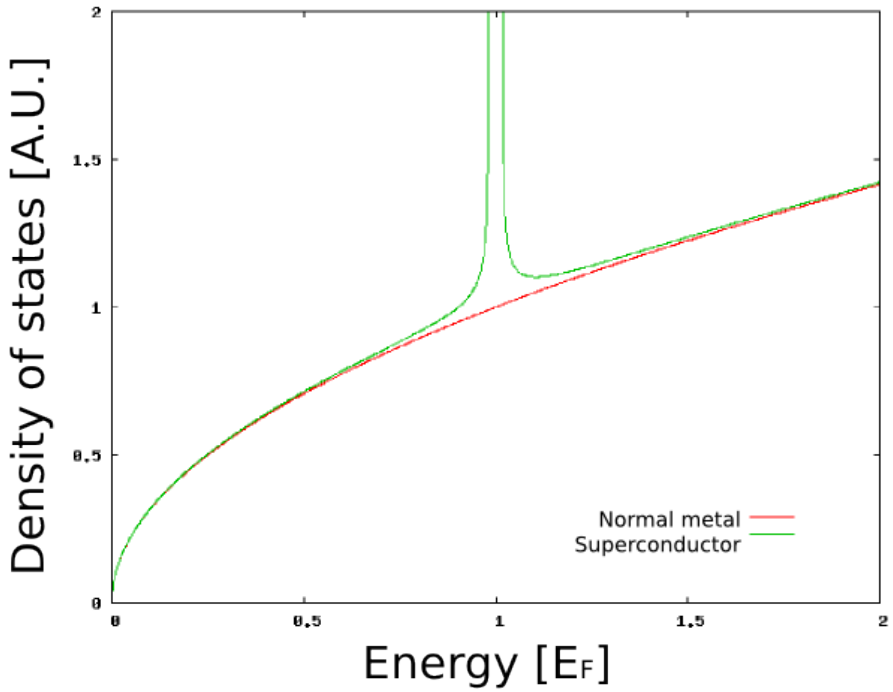

Figure 1.1: Density of stationary states as a function of energy in a normal metal and in a superconductor. For the latter no states exist with energy $E_F - \Delta < E < E_F + \Delta$.

In a small interval around the Fermi energy E_F, the DOS is zero. Let the half-width of this interval be Δ. The electrons of every material at zero temperature occupy the lowest energy levels. In a superconductor, this happens up to $E_F - \Delta$. Beyond this value, only states with energy greater than $E_F + \Delta$ are available. If all single-electron stationary states up to $E_F - \Delta$ are occupied, the finite energy gap originates two effects:

1. electrons in these states cannot be subject to small interactions with the environment, because the smallest energy required to change their state is finite and equals 2Δ;

2. electrons make bound states. They form pairs with binding energy 2Δ, instead of occupying high-energy single-particle states.

We note that the presence of the finite energy gap qualitatively explains both experimental evidences of superconductivity. Neither single electrons in the Fermi sphere nor electon pairs can scatter, because the energy involved in typical system-environment interactions is smaller than 2Δ; the

resistivity of a superconducting material vanishes. Moreover, magnetic fields are excluded from a bulk superconductor, because of a Lenz-type shielding supercurrent on the surface of the superconductor. Since the resistivity for this current is actually zero, the magnetic shielding is perfect.

1.4.2 Electron-electron interaction mechanisms

The reader may wonder how charged particles of equal sign like electrons are able, in spite of their mutual electrostatic repulsion, to form bound states. The answer to this question is the very core of the theory of superconductivity.

The first successfull microscopical theory of superconductivity is the *BCS theory*[7]. In that context, the direct electron-electron repulsion is screened by phonons of the crystal lattice. In simple words, a moving electron emits a phonon, which is then captured by another electron. The travelling phonon alters the lattice geometry in such a way that it can be interpreted as a moving positively charged particle. The resulting indirect interaction is effectively attractive.

This elucidation holds for all pure superconducting materials and even for some alloys, but fails to predict properties of high-temperature superconducting alloys like Yttrium barium copper oxide (YBCO). For these materials no definitive theory has been developed yet, though the so-called *d-wave pairing theories* are thought to be on the right track.

1.4.3 Cooper pairs and their BEC

Whatever the binding mechanism could be, electrons are experimentally seen to move in pairs. They are also known as *Cooper pairs*[7]. These pairs, like every structure composed by an even number of fermions, behave like bosons. They can condens into the lowest energy or *ground state*, in a process called *Bose-Einstein Condensation* (BEC). All pairs in this stationary state have energy $2E_F$ and can be thought as lying on the Fermi surface of the single-particle space of momenta.

It is important to remark, that Cooper pairs are *not* real bosons, in the sense that their spectrum has no excited states. Pairs are always in the ground state; the bond energy is smaller than the energy difference between first hypothetical excited state and ground state. If a pair gets sufficient energy, it splits into single particles. Since the energy of a pair is $2E_F$, a minimal energy of 2Δ is needed to break a pair[4]. Thus Cooper pairs can not slightly interact with the environment and are able to remain in a quantum state, the ground state, for long lifetimes.

[4]Both electrons have to get into the $E_F + \Delta$ high-energy state.

Charge of the Cooper pairs

Cooper pairs, as long as they remain in the ground state, are studied as single bosons. Their charge is twice that of one electron, thus the voltage-energy conversion for pairs is:

$$\Delta E = -2e\Delta V \tag{1.6}$$

In the next chapter we will almost always use ΔE as a variable, to stress the generality of our formulation of the Josephson theory. This generality is a key component of the recent research projects explained in the last chapter.

1.4.4 Critical temperature and critical magnetic field

The appearance of superconductivity depends on the thermodynamic conditions. Both high temperature and intense magnetic field can destroy superconductivity. Using the Ginzburg-Landau theory[8][6, 41], it is possible to show that the superconducting phase is stable for magnetic fields and temperatures smaller than a certain transition curve $H_c = H_c(T_c)$. The analytical form of this line, near the zero-field critical temperature T_c, is just:

$$H_c \propto (T_c - T)$$

From a purely thermodynamic point of view, it is interesting to remark that the superconducting transition is first-order for nonvanishing magnetic fields, while it becomes second-order in the limit $T \to T_c$.

The BCS theory calculates also the temperature dependence of Δ[6, 74]. This turns out to be zero above T_c and to increase continuously below this temperature. Near the transition it holds:

$$\Delta(T) = 3.06kT_c \left(1 - \frac{T}{T_c}\right)^{1/2}$$

This means that superconductivity can only take place at low temperatures, where the energy gap is strictly greater than zero.

1.4.5 Macroscopic wavefunction of pairs

The ground state of electron pairs is a really quantum one, thus it can be described by a wavefunction ψ. Its square module represents the density of Cooper pairs, while its phase is connected with their movement:

$$\psi = \rho^{1/2}\, e^{i\varphi} \tag{1.7}$$

The spatial coherence of the macroscopic wavefunction deserves a dedicated discussion. In our theoretical picture, we only dealt with momentum

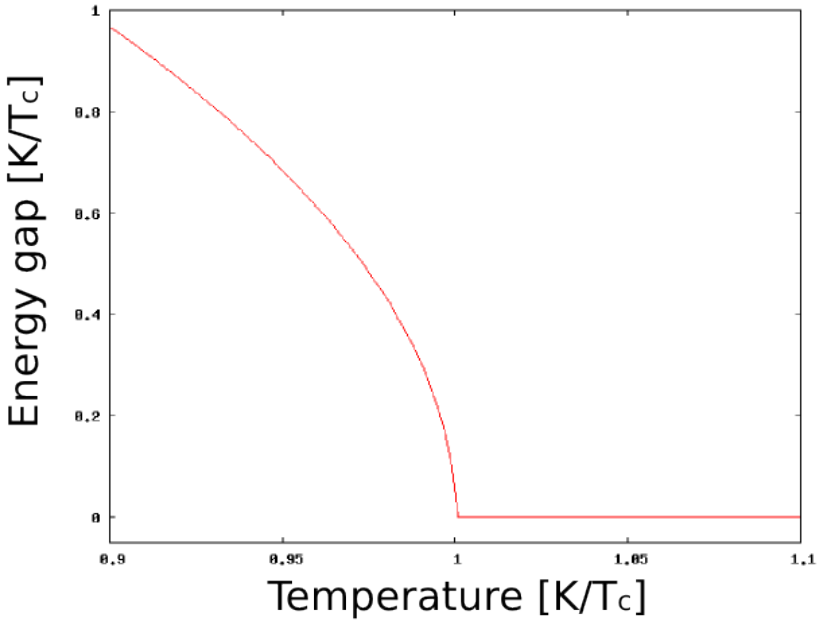

Figure 1.2: Analytical plot energy gap against temperature in a simple superconductor, according to the BCS theory.

and energy, but it's clear that electrons can not form bound states if they are too far away from each other. As a matter of fact, the pair wavefunction shows an intrinsec typical length which limits its coherent behaviour. This is called *coherence length* and is, in classic superconductors like Niobium, of the order of ~ 10 nm.

The electric current can be calculated from (1.7) using the standard formula of quantum mechanics (1.5)[5]:

$$\begin{aligned}\mathbf{J} =& \frac{2e}{2m}\left[\frac{i\hbar}{2}\left(\psi\nabla\psi^* - \psi^*\nabla\psi\right) - 2e\mathbf{A}\left|\psi\right|^2\right] \\ =& \rho\frac{e}{m}\left(\hbar\nabla\varphi - 2e\mathbf{A}\right)\end{aligned} \tag{1.8}$$

The key point of this equation is that a measurable quantity, the current density, is directly connected to the phase of the wavefunction describing the quantum state of Cooper pairs. Thus quantum macroscopic effects due to φ can be observed through current measurements. This is the essence of the Josephson effect, which we analyze more deeply in the next chapter.

[5]Strictly speaking, the following equation is valid only for superconductors with cubic crystal symmetry. In general, the electric current can have another direction than the velocity of pairs. See [6, 32].

Chapter 2

Josephson effect and junctions

The Josephson effect is in fact a collection of different phenomena, which originate from interference between two superconductors' macroscopic wavefunctions. The practical device, in which these effects take place, is the *Josephson junction* (see fig. 2.1). It consists of a thin layer (~ 10Å) of insulating material, placed between two superconductors. It is also called tunnel junction or SIS (Supercontuctor-Insulator-Superconductor) junction. Similar effects are found with non-insulating materials, but the theory is more difficult. Whatever the nature of the junction, its thickness has to be comparable or smaller than the coherence length of the two superconductors. Otherwise the dynamics of the respective Cooper pairs are uncorrelated.

In the following section, we show the core two-state theory of the Josephson effect. In the second part, a simple model for a SIS junction is given. Equation governing the dynamics of a junction is then presented. In the last section, experimental data, collected by some colleagues and me, are presented.

2.1 Two-state theory

We restrict our analysis to the easier case of a SIS junction. Josephson himself assumed the same condition in his original paper[2]. However, for the sake of mathematical simplicity we do not follow the approach of Josephson. We use the two-state picture instead, as proposed by Feynman[1]. This choice has also a very useful physical advantage: generality. In chapter 3, we discuss some applications of the two-state theory in superfluids and in cold atomic gases.

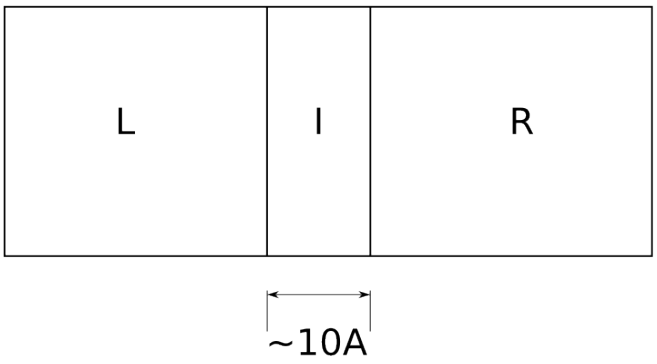

Figure 2.1: Schematic representation of a Josephson junction. **L** and **R** can be made of the same material, as well as of different superconductors.

In this section, we discuss only the contribution of tunneling Cooper pairs. We neglect single-electron tunneling, and exclude the possibility of a dielectric breakdown of the insulating layer. A complete model of the junction, which is given in section 2.2, is necessary to understand the experimental I-V curves. These data are shown and explained in section 2.3.

Let **L** and **R** be respectively two insulated superconductors. Let then ψ_L (ψ_R) be the macroscopic wavefunctions of the left (right) superconducting electrons. In the absence of interaction between the superconductors, the evolution is described through ordinary Schrödinger equations:

$$i\hbar\frac{\partial\psi_L}{\partial t} = \mathbf{H}_L\psi_L \tag{2.1}$$

$$i\hbar\frac{\partial\psi_R}{\partial t} = \mathbf{H}_R\psi_R \tag{2.2}$$

In a stationary situation we have $\mathbf{H}_k\psi_k = E_k\psi_k$.

Now, let the superconductors be brought towards each other. At a certain distance, of the order of nanometers, they start to 'feel' each other because of the coherence lenght of their wavefunctions. We can introduce the coupling between them, in a simple but powerful manner, by writing the

new evolution equations:

$$i\hbar\frac{\partial\psi_L}{\partial t} = E_L\psi_L + K\psi_R \tag{2.3}$$

$$i\hbar\frac{\partial\psi_R}{\partial t} = E_R\psi_R + K\psi_L \tag{2.4}$$

where K is a phenomenological parameter which describes the properties of the insulating barrier. Now introducing the general form of the macroscopic wavefunction:

$$\psi_k = \rho_k^{1/2} e^{i\varphi_k}$$

we obtain:

$$\frac{\partial\rho_L}{\partial t} = \frac{2}{\hbar}K\sqrt{\rho_L\rho_R}\,\sin\Delta\varphi \tag{2.5}$$

$$\frac{\partial\rho_R}{\partial t} = -\frac{2}{\hbar}K\sqrt{\rho_L\rho_R}\,\sin\Delta\varphi \tag{2.6}$$

$$\frac{\partial\varphi_L}{\partial t} = -\frac{K}{\hbar}\sqrt{\frac{\rho_R}{\rho_L}}\,\cos\Delta\varphi - \frac{E_L}{\hbar} \tag{2.7}$$

$$\frac{\partial\varphi_R}{\partial t} = -\frac{K}{\hbar}\sqrt{\frac{\rho_L}{\rho_R}}\,\cos\Delta\varphi - \frac{E_R}{\hbar} \tag{2.8}$$

where $\Delta\varphi := \varphi_L - \varphi_R$ and $\Delta E := E_L - E_R$. The current density is just given by $J := 2e\partial\rho_L/\partial t$, thus we find:

$$J = \frac{4eK}{\hbar}\sqrt{\rho_L\rho_R}\,\sin\Delta\varphi \tag{2.9}$$

This expression is quite involved. However, because of periodicity of the phase difference, the current density can be expanded in a Fourier serie. The current density has to be an odd function of $\Delta\varphi$ because of antisymmetry under exchange of **L** and **R**; all cosinus terms vanish:

$$J = \sum_{k=1}^{\infty} J_k \sin(k\Delta\varphi) \tag{2.10}$$

2.1.1 Josephson equations

In first approximation we can suppose that

$$\rho_L \approx \rho_R \approx constant =: \rho \tag{2.11}$$

This is a physically reasonable assumption. It means that our bulk electrodes have an overwhelming quantity of Cooper pairs which do not tunnel through the junction. It immediately follows from (2.10) that:

$$J = J_c \sin\Delta\varphi \qquad \textbf{First Josephson equation} \tag{2.12}$$

where $J_c := 2K\rho/\hbar$ is the so-called *critical current density*. In the same approximation it results:

$$\frac{\partial \Delta\varphi}{\partial t} = -\frac{\Delta E}{\hbar} \qquad \textbf{Second Josephson equation} \tag{2.13}$$

We stress that approximation (2.11) is a necessary requirement for these relation. Without this hypothesis, the core equation (2.10) of our theory would be much more difficult to handle.

The total current flowing through the junction can be calculated through spatial integration of (2.12). Whether this is an easy task or not depends on the junction geometry. The easiest case is when the junction is small. In that case, impurities and surface effects can be completely neglected and we find:

$$I = I_c \sin \Delta\varphi$$

In the more general situation of finite dimensions, things get much more intricate. For instance, one has to take into account that supercurrents, except for the junction area, actually flow within a thin layer on the surface. Current density at the junction border is probably not homogeneous, and the above integration becomes difficult.

2.1.2 DC Josephson effect

A first insight into the variety of the Josephson effects comes from the zero voltage behaviour. When the energy difference between **L** und **R** is zero, using (2.12) and (2.13) we find:

$$J = J_c \sin \Delta\varphi_0 \quad \Longrightarrow \quad |J| < J_c$$

This current is purely of quantum nature and follows only from the phase difference $\Delta\varphi_0$. There is an evident analogy with bulk superconductors, in which the supercurrent is determined by phase gradients[9, 12]. Now the name "critical current density" has become clear: it is the maximum value of J through the junction in absence of an energy difference.

It is possible to feed a Josephson junction with a high current density $J > J_c$. The Cooper-pairs current density, or supercurrent density, is the only zero-voltage contribution, and that can not exceed J_c. Therefore, a feed current $J > J_c$ makes a voltage difference appear across the junction (see section 2.3).

2.1.3 AC Josephson effect

The two Josephson equation described above show other interesting features when a constant energy difference is established through the junction. From

(2.13) we get $\Delta\varphi = \Delta\varphi_0 + \omega_E t$ with $\omega_E := -\Delta E/\hbar$. Injecting this into (2.12) gives:

$$J = J_c \sin\left(\Delta\varphi_0 + \omega_E t\right) \tag{2.14}$$

The relation (2.14) shows that a Josephson junction is an *ideal voltage-frequency converter*. In other words, a tunnel junction fed with a constant voltage shows a current that oscillates with a constant frequency.

2.1.4 Shapiro current steps

If the junction is driven by an alternating energy difference, characteristical current (density) steps appear in the I-V curve. Let ΔE be of the form:

$$\Delta E = \Delta E_0 + \epsilon \cos\omega_r t$$

then the phase difference is given by:

$$\Delta\varphi = \omega_{E_0} t + a \sin\omega_r t + \Delta\varphi_0$$

where a and ω_{E_0} are defined through:

$$a := \frac{\omega_{E_0}}{\omega_r}\frac{\epsilon}{\Delta E_0} \qquad \text{and} \qquad \omega_{E_0} := -\frac{\Delta E_0}{\hbar}$$

The current density is:

$$\begin{aligned} J =& J_c \sin\left(\omega_{E_0} t + a\sin\omega_r t + \Delta\varphi_0\right) \\ =& J_c\Big[\sin\left(\omega_{E_0} t + \Delta\varphi_0\right)\cos\left(a\sin\omega_r t\right) + \cos\left(\omega_{E_0} t + \Delta\varphi_0\right)\sin\left(a\sin\omega_r t\right)\Big] \end{aligned}$$

It is possible to expand the double trigonometric functions in Fourier-Bessel series[9, 292]. After some algebraic simplification we get a final expression:

$$\begin{aligned} J = J_c\Big\{ & J_0(a)\sin\left(\omega_{E_0} t + \Delta\varphi_0\right) + \\ + \sum_{l=1}^{\infty} & J_l(a)\left[\sin\left(\left(l\omega_r + \omega_{E_0}\right)t + \Delta\varphi_0\right) - (-1)^l \sin\left(\left(l\omega_r - \omega_{E_0}\right)t + \Delta\varphi_0\right)\right]\Big\} \end{aligned} \tag{2.15}$$

in which J_l is the l-th Bessel function of first kind. This sum is composed of many sinus functions of time with different frequencies. Since the sinus is a zero-mean function, the supercurrent density has a DC component only when at least one frequency is zero. This corresponds to:

$$\Delta E_0 = n\hbar\omega_r \qquad \text{with } n \in \mathbb{Z} \tag{2.16}$$

It is also self-evident that no more than one frequency can be zero. Thus the time average of the current is given by:

$$\bar{J} = J_c \cdot J_n(a_n)\sin\Delta\varphi_0$$

The I-V curves, which describe all current components, show a staircase pattern with steps at $n\hbar\omega_r$. These steps are called *Shapiro steps*[10], and are due to Cooper pairs tunneling. Out of the energy steps $n\hbar\omega_r$, the supercurrent has zero mean, and the I-V curve is determined by other current components. Experimental curves are shown in section 2.3.

2.1.5 Magnetic field effects

Until now we have only examined the behaviour of a SIS junction in absence of magnetic fields. If a magnetic field is present, equations (2.12) and (2.13) are not correct, because they are not gauge invariant. The physics of the Josephson effect can not depend on a particular gauge choice for the electromagnetic potentials. The phase difference in its gauge invariant form is:

$$\Theta := \Delta\varphi + \frac{2e}{\hbar}\int_{z_L}^{z_R} \boldsymbol{A}\cdot \mathrm{d}\boldsymbol{s}$$

where z is the direction of the junction axis. This definition is coherent with expression (1.8) for the gauge invariant phase gradient in a bulk superconductor.

The *gauge invariant Josephson equations* are:

$$J = J_c \sin\Theta \tag{2.17}$$

$$\frac{\partial\Theta}{\partial t} = -\frac{\Delta E}{\hbar} \tag{2.18}$$

Now, let us assume that the supercurrent density is directed, inside the junction, along z. This is equivalent to the hypothesis, that the junction is small and homogeneous. Let the magnetic field be perpendicular to the junction axis, say along y direction: $\mathbf{H} = -|\mathbf{H}|\,\mathbf{e_y}$. We investigate the spatial dipendence of the Josephson current in the x direction. Applying equation (1.8) to both the left and right side of the junction and integrating the left and right side fields along the contours shown in figure 2.2, we find:

$$\varphi_i(x_2) - \varphi_i(x_1) = \frac{2e}{\hbar}\int_{C_i}\left(\frac{m}{2e^2\rho}\mathbf{J} + \mathbf{A}\right)\cdot \mathrm{d}s$$

where $i = L, R$ is the side of the barrier. Subtracting the right side equation from the left side one:

$$\Delta\varphi(x_2) - \Delta\varphi(x_1) = \frac{2e}{\hbar}\left[\int_{C_L}\left(\frac{m}{2e^2\rho}\mathbf{J} + \mathbf{A}\right)\cdot \mathrm{d}s + \int_{-C_R}\left(\frac{m}{2e^2\rho}\mathbf{J} + \mathbf{A}\right)\cdot \mathrm{d}s\right]$$

with obvious notation. We know that the supercurrent $\mathbf{J}$ of a superconductor must flow on its surface and parallel to it. Thus we can choose the contours C_i, so that they are orthogonal to $\mathbf{J}$ in the penetration region. The vertical

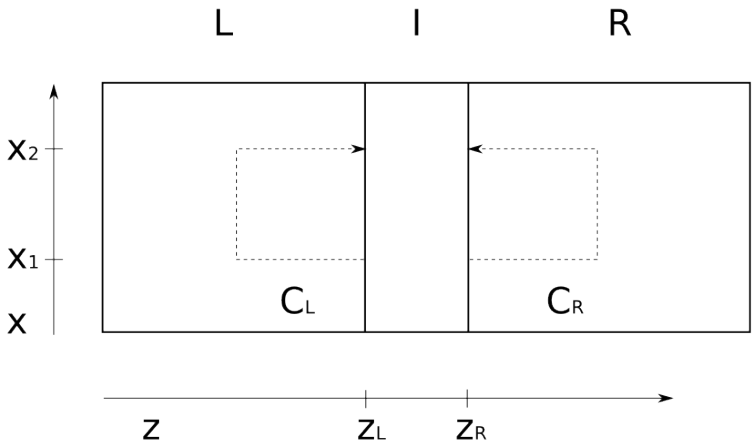

Figure 2.2: Schematic representation of a small Josephson junction in a magnetic field. The direction of the field is y. C_L and C_R are the contours of integration.

region is deeply inside the superconductors, where the supercurrent vanishes. As a consequence, **J** does not influence the integration:

$$\Delta\varphi(x_2) - \Delta\varphi(x_1) = \frac{2e}{\hbar}\int_{C_L} \mathbf{A}\cdot \mathrm{d}s + \int_{-C_R} \mathbf{A}\cdot \mathrm{d}s$$

Introducing at this point the gauge invariant phase difference Θ we find:

$$\Theta(x_2) - \Theta(x_1) = -\frac{2e}{\hbar}\oint \mathbf{A}\cdot \mathrm{d}s$$

Furthermore, using the elementary version of Stokes' theorem and assuming a London-like exponential decay of the magnetic field inside the bulk superconductors we get the final result:

$$\Theta(x) = \frac{2e}{\hbar} dHx + \Theta_0 \tag{2.19}$$

with $d := d_0 + \lambda_{\mathbf{R}} + \lambda_{\mathbf{L}}$. d_0 is the material thickness of the junction, and λ_i is the so-called *magnetic penetration depth*. This quantity is an estimate for the thickness of the surface layer, where magnetic fields are able to flow. The term Θ_0 represents the border conditions of the junction. The current

density follows from the first gauge invariant Josephson equation:

$$J = J_c \sin\left(\frac{2e}{\hbar} dHx + \Theta_0\right) \tag{2.20}$$

The supercurrent density is sinus-modulated by the intensity of **H**. It is interesting to remark that, even if the junction is assumed homogeneous, the current density is not. In a less simplified approach, this is not surprising, since neither the junction nor the current are homogeneous.

The total Josephson current is given by integraton of **J**. It is an oscillating function of H. Its form is shown in figure 2.8, and has an evident Fraunhofer-like diffraction pattern; the quantum nature of the Josephson effect is clear. The role of photons in optical diffraction is taken by superconducting electron pairs. The fundamental intuition of de Broglie[11] is unavoidably verified by these experimental data.

2.2 Simple model of a tunnel junction

In this section we discuss a simple but realistic model for the Josephson junction. Its main assumption is that the dynamics can be studied by splitting the total current into discrete components, which account for diffent physical phenomena. In a metal, even at zero temperature, not all electrons are in the Cooper pairs ground state. Some electrons flow resistively through the junction and contribute with a normal current I_N. A displacement current I_D has also to be taken into account, for the barrier is insulating and acts as a capacitor. Finally, there are noise currents I_F. The simplest complete equation describing the electodynamics of the junction is therefore[12, 18]:

$$I = I_S(\Delta\varphi) + I_N(V) + I_D(\dot{V}) + I_F(t) \tag{2.21}$$

The supercurrent I_S can be found applying the first Josephson equation. The other component will be studied in the following. We note that an easy equivalent circuit for the SIS junction does exist in our model[12, 18] (see fig. 2.3).

It is not obvious that this circuit approximates well a real Josephson junction. All electrical features of a Josephson junction should be described by means of a distribute, microscopically justified model. Actually, microscopically derived (like the *TJM model*[12, 49]) and distributed models[12, 271] of the Josephson junction have been studied. They will not be discussed here because of their high complexity.

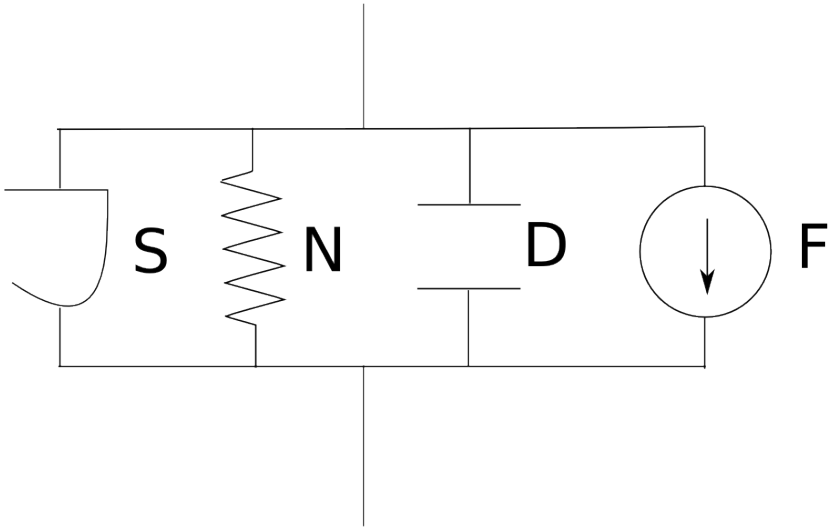

Figure 2.3: Electric scheme for the discrete model of the Josephson junction. The components are, from the left the following: purely superconducting junction (**S**), resistor (**N**), capacitor (**D**) and noise (**F**).

2.2.1 Normal current

The normal current is formed by single non-superconducting electrons, which are driven to tunnel through the junction by a voltage difference across it. There are two sources for these.

Thermal fluctuations can excite some electrons out of the superconducting state if their mean energy is comparable with the superconducting state bond energy of the electrodes, that is $kT \sim \Delta(T)$. The excited electrons dissipate energy by passing the junction. Since $\Delta(T)$ is a continuous, decreasing function of temperature till $\Delta(T_c) = 0$, this mechanism becomes more important with increasing temperature. There are two simple cases:

- at high temperatures $T \sim T_c$, almost all electrons of the electrodes are in this excited or normal state, thus the junction basically behaves like a resistor with resistance $R_N := I_N/V$;
- if the energy imbalance across the junction exceeds the sum of the bond energies of both electrodes, $\Delta E > \Delta_L(T) + \Delta_R(T)$, the superconducting electron pairs break up and one electron passes directly through the junction. If ΔE is kept constant by an external power source, all pairs are disrupted in a short time and the junction shows

again resistive characteristics;

In the other cases, when the two conditions above are not fulfilled, the modelling of I_N becomes more complicated. Historically, different approaches have been chosen to stress either simplicity or precision. The simplest is the so-called *RSJ model* developed by McCumber[13] and Stewart[14], which assumes that the linear dipendence $I_N(V) = V/R_N$ holds in all circumstances. In a successive improvement, proposed by Scott[15], a piecewise-linear approximation for I_N is assumed:

$$I_N(V) = V \times \begin{cases} 1/R_L & \text{at } |V| < V_g, \\ 1/R_N & \text{at } |V| > V_g. \end{cases}$$

where $V_g := [\Delta_L(T) + \Delta_R(T)]/e$ is the threshold voltage for the second condition above and R_L is a phenomenological low-voltage resistance (usually taken between $5R_N$ and $20R_N$[12, 48]). The precision of the model can be further increased by choosing for I_N a better function such as:

$$I_N(V) = \frac{V}{R_N} \cdot \frac{(V/V_g)^n}{1 + (V/V_g)^n} \qquad \text{with } n \gg 1$$

Alternatively, a numerical model for I_N can be adopted (see sec. 2.3.1). If the $I_N(V)$ dependance is not linear, the model is called *RSJN model*. Its main disadvantage is its mathematical complexity, for which it is often necessary to rely on numerical computations.

2.2.2 Displacement current

This component comes from the electrical field established through the junction because of its insulation. As explained by Likharev[12, 13], it is normally sufficient to attribute a capacity C to the junction and accept the ordinary capacitor equation:

$$I_D = C\dot{V}$$

Since a simple capacitor is basically a high-pass filter, it is clear that I_D becomes increasingly important for high-frequency signals through the junction. In the zero-frequency limit, that is when ΔE is constant in time, the displacement current is not present at all.

2.2.3 Noise current

The noise current I_F is intended to describe the varous fluctuations af a Josephson junction in a Langevin-like fashion. I_F is a random force, whose origins will be studied qualitatively. For a quantitative formulation of this issue see e.g. [12].

The noise sources in a junction are *thermal noise*, *shot noise*, $1/f$ *noise*, *external noise* and *quantum noise*.

Thermal noise is generated from the resistive component of the junction and is of major importance if:

$$kT \gg \Delta E, \hbar\omega$$

where ΔE is the energy imbalance across the junction and ω is the studied noise frequency.

Shot noise is important if following condition is satisfied:

$$\Delta E \gg kT, \hbar\omega$$

Its origin is in the finite number of charge carriers (electrons) through the junction.

Pink or $1/f$ noise is visible only at very low frequencies. Since the voltage-frequency conversion of a junction links meV energies with GHz frequencies, this source can almost always be neglected.

External noise is given by interferences between the junction and the external world, that is radio and TV stations, electrical transmission lines and so on.

Quantum noise is of great importance at very high frequencies, that is when:

$$\hbar\omega \gg kT, \Delta E$$

and is caused by Heisenberg uncertainty principle for phase and particle number. It results $\Delta(\Delta\varphi)\cdot\Delta(\Delta N) \geq 1$ where ΔN is deviation of the electron number in superconducting state from electrical equilibrium. Although the very basics of these fluctuations are of quantum nature and can only be explained by quantum calculations, it has been shown (see [12, 21] and references therein) that they can be described together with other classical noises in a Langevin-like way through I_F.

2.2.4 Relative importance of the currents and damping

As written in section 2.2.1, the relative intensity of I_N and I_S depends on the voltage across the junction and on the temperature. The higher one of these parameters (or both), the bigger the contribution of the normal current. In the resistive limit one finds the normal state resistance R_N and can therefore define a *critical frequency* of the junction:

$$\omega_c := \frac{\Delta E_c}{\hbar} \qquad \text{with} \qquad \Delta E_c := 2eI_cR_N$$

The importance of I_D, because of its capacitive character, changes with the frequency. Defining the *RC-frequency* as:

$$\omega_{RC} := \frac{1}{R_N C}$$

and the *plasma frequency* of the junction as:

$$\omega_p := \left(\omega_{RC} \cdot \omega_c\right)^{1/2}$$

it is possible to show[12, 14] following relations:

$$\begin{aligned} I_D &\gtrsim I_S \quad \text{if} \quad \omega \gtrsim \omega_p \quad \text{and} \\ I_D &\gtrsim I_N \quad \text{if} \quad \omega \gtrsim \omega_{RC} \end{aligned}$$

At very high frequencies the capacitive part of the current is the most important. However, one must consider that a Josephson junction can not operate at frequencies higher than ω_c because of its inner relaxation times. A typical value for $\omega_c/2\pi$ is around 10^{12} Hz.

The dynamics of a Junction can show a more or less capacitive character, depending on the values of C, R_N and I_c. A dimensionless parameter which describes this feature is the so-called *McCumber parameter*:

$$\beta = (\omega_c/\omega_p)^2 = (2e/\hbar) I_c R_N^2 C$$

Junctions with $\beta \ll 1$ are called *highly damped*, while junction with $\beta \gg 1$ are referred as *lowly damped*.

2.2.5 Dynamics equation

The role of the McCumber parameter is clear if we rewrite equation (2.21) in a different form. Defining the auxiliary variables:

$$\tau := \frac{2eI_cR}{\hbar}t \quad , \quad i := \frac{I}{I_c} \quad \text{and} \quad f := \frac{I_F}{I_c}$$

and using formulae (2.17) and (2.18), we obtain the dynamics equation for our junction model:

$$i = sin\Theta + \frac{\mathrm{d}\Theta}{\mathrm{d}\tau} + \beta\frac{\mathrm{d}^2\Theta}{\mathrm{d}\tau^2} + f(\tau) \tag{2.22}$$

In the high damping limit, the junction shows a very rapid reaction to external variations. On the contrary, in low damping situations the junction shows a long transient behaviour. Equation (2.22) is the key mathematical relation explaining the experimental data of the next section.

2.3 Experimental data

In this section we see some experimental data collected in 2008 by Teresa Selistrovski, Georg Kurij, Alexander Opitz, and me at Universität Tübingen, Germany. This work was part of a laboratory-oriented class.

The experimental setup was entirely planned and realized by the research group of Prof. Dr. Kölle and Prof. Dr. Kleiner. It consisted of a few Nb–AlO_x–Nb Josephson junctions placed on a silicon chip. This probe was immersed in a liquid helium container at $\sim$ 4 K, surrounded by a liquid nitrogen bath at $\sim$ 77 K. The junctions were fabricated through standard trilayer technology, which involves following processes:

- sputtering for Nb layers deposition;
- plasma chemical vapor deposition for SiO_2 formation;
- photolithography for junction tailoring.

This techique made it possible to store several junction on a single chip. The junctions had different McCumber parameters. This effect was obtained by putting different shunt resistances in parallel with the junctions. Here we analyze three junctions, with $\beta_1 \gg \beta_2 \gg \beta_3$. According to equation (2.22), their dynamics are expected to be quite different.

2.3.1 I-V curves

The following three images refer to current-fed, magnetic field-free Josephson junctions. For the last plot, one of the junction was brought into an electromagnetic field. The current scan time was around one minute.

In the low-damping case of junction 1, the supercurrent component of the dynamics equation (2.22) can be safely neglected at any nonvanishing voltage. In a quasi-stationary situation, the displacement component is also small. The I-V curve is just that of single electron tunneling. It can also be acquired with a computer to build a precise numerical model for I_N. Obviously, at zero voltage the supercurrent is not negligible, because it is the only contribution left. Our experimental data are shown in figure 2.4.

In the high-damping case of junction 3, it is the capacitive term which can be cut away from (2.22). The resulting equation can be analytically solved in the absence of noise (see [12, 92] and references therein):

$$V(I) = R_N \cdot \operatorname{sgn}(I) \cdot \left(I^2 - I_c^2\right)^{1/2}$$

This curve is a signed hyperbole. Our measurements are reported in figure 2.5.

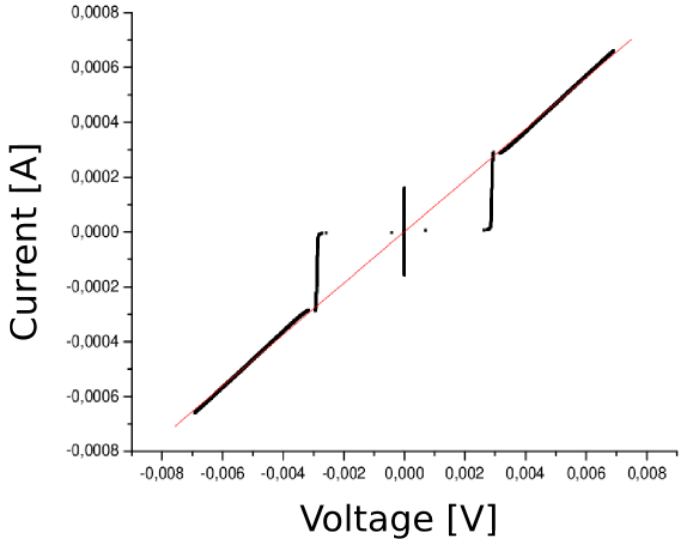

Figure 2.4: Current-voltage curve for junction 1 (low damping). The zero voltage peak is a clear manifestation of the DC Josephson effect. The rest of the graphic shows the I_N-V dependence, which is strongly nonlinear for currents $I \lesssim I_c$.

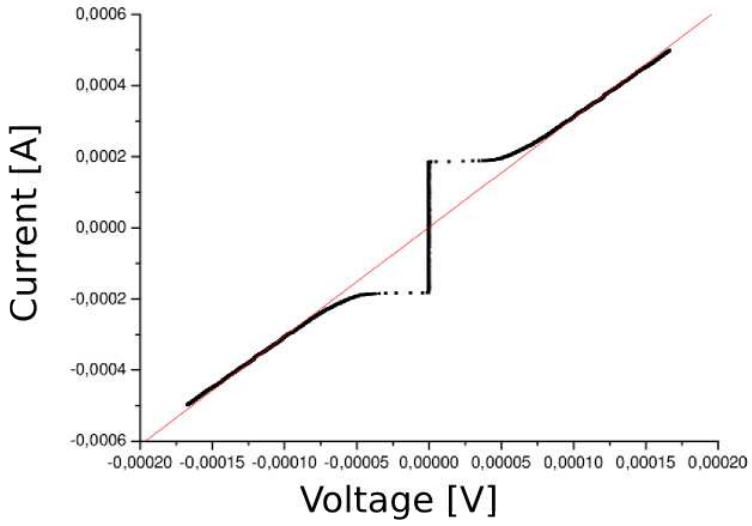

Figure 2.5: Current-voltage curve for junction 3 (high damping). The hyperbolic shape of the curve is clearly visible. The DC Josephson peak is also present.

In the intermediate case of junction 2, the dynamics equation has to be solved numerically. At a qualitative level, an intermediate behaviour between figures 2.4 and 2.5 is expected. This is exactly what we observed in our experiment, as illustrated in figure 2.6.

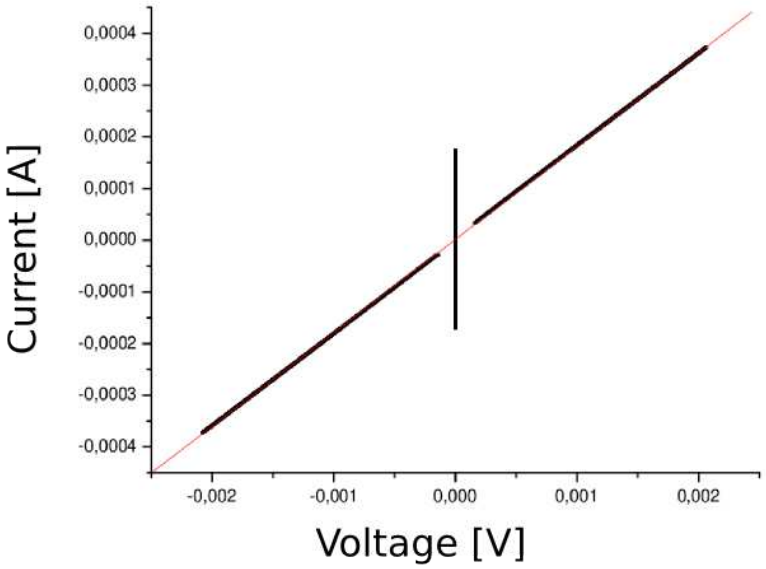

Figure 2.6: Current-voltage curve for junction 2. The quasiparticle curve is observable down to currents smaller than I_c. At some point, depending on β, the curve is numerically predicted to approximate the hyperbolic shape. This is not visible in our figure because of the lack of experimental points in that region.

Figure 2.7 is a plot of the I-V curve of a Josephson junction irradiated through a microwave elentromagnetic field. The theoretical prediction of equation (2.16) is confirmed.

2.3.2 I-H curves

We have also measured the current vs magnetic field behaviour predicted by spatial integration of equation (2.20). As explained in the previous section 2.1.5, a diffraction pattern is observed. The curves of the three junctions are very close to each other. This is in accordance with the theoretical result of (2.20), in which the McCumber parameter does not play any role.

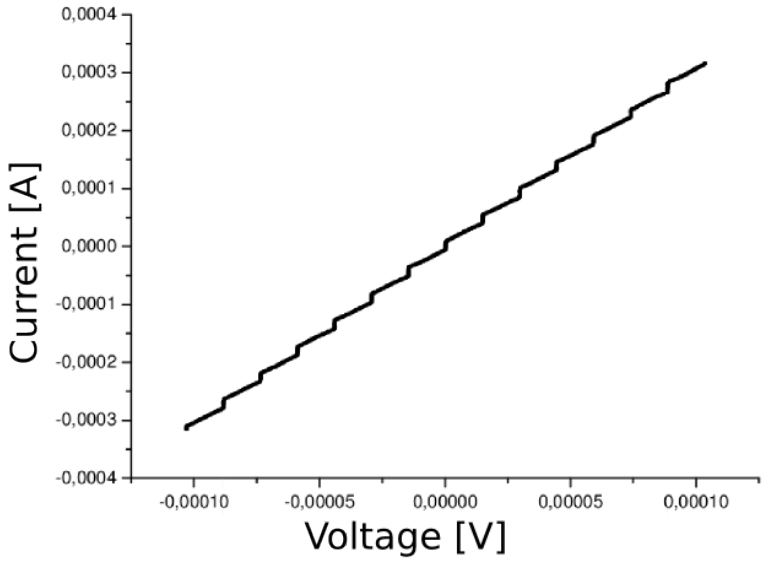

Figure 2.7: Current-voltage curve for a Josephson junction in a microwave electromagnetic field. The Shapiro steps are evident.

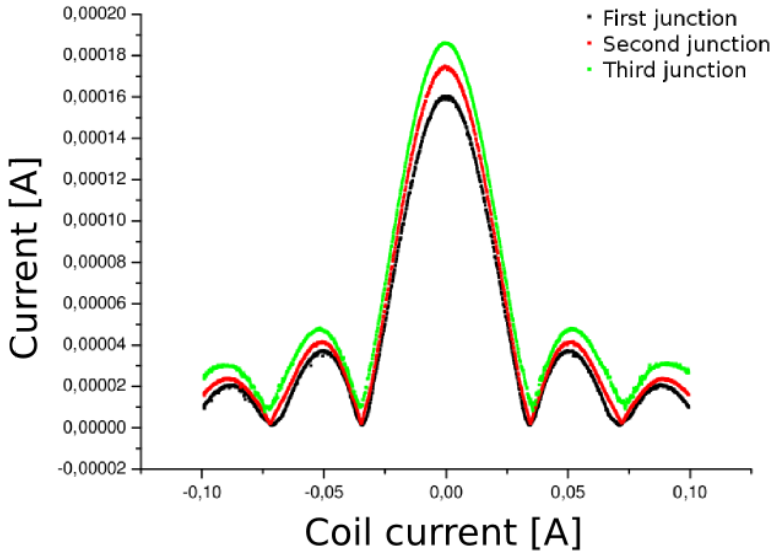

Figure 2.8: Josephson junction immersed in a magnetic field, generated through a large-current coil. This is the coil current-junction current curve. The diffraction pattern is evident.

Chapter 3

Applications and recent progresses

The junctions studied by Josephson[2] were tunnel junctions. In these junctions the barrier consists of an insulating layer[1], whence their name *Superconductor-Insulator-Superconductor* (SIS) *junctions* . It is possible to build other types of junctions, called in general *weak links*. Nowadays, the name "Josephson junction" is used as well to indicate a weak link. There are many kinds of weak links, for instance *Superconductor-Normal metal-Superconductor* (SNS) and even more complex structures (SNIS, SINIS, etc.). Their phenomenology is generally more complicated and worse known than that of the SIS. After the discovery of *high-T_c superconductivity*[16], many studies on high-T_c weak links have been made. The same is true for Superconductor-Ferromagnet-Superconductor or SFS junctions (see e.g. [17]).

It is impossible, in this thesis, even to touch those topics, because of both an extremely rich phenomenology and absence of a general theory. In the following, a brief summary of the most important applications of the "classical" SIS junctions is presented. The last paragraph is a short overview of Josephson-like phenomena recently found in other quantum fluids, i.e. superfluids and atomic gases.

3.1 Applications of the Josephson effect

The Josephson effect is certainly a stimulating topic of research in both experimental and theoretical physics, but also a source of widely used practical applications. A short but impressively dense review on the subject can be found in [18].

[1] The insulator is typically an oxide like AlO or NbO.

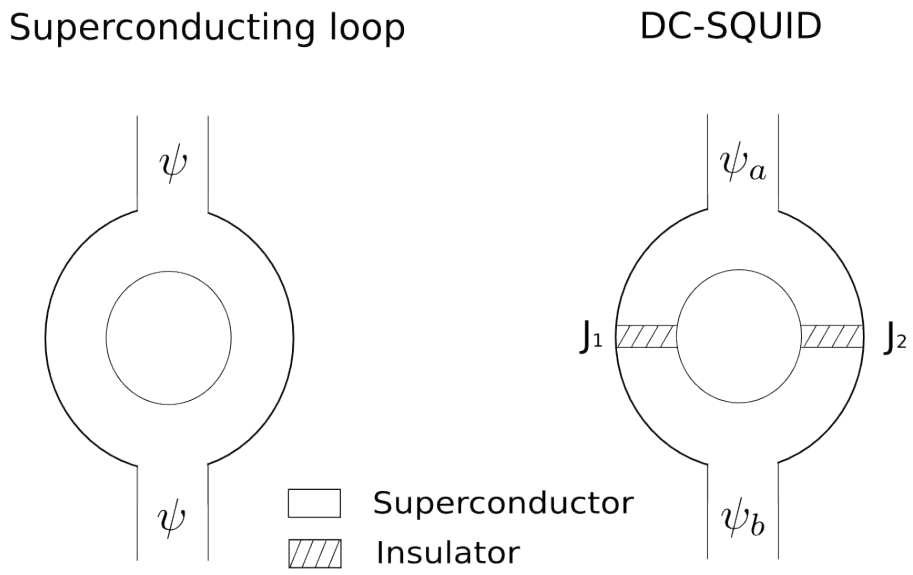

Figure 3.1: Schematic representation of a superconducting loop and a DC-SQUID.

3.1.1 SQUIDs

An important application is the Superconductive QUantum Interference Device (SQUID). It is essentially a superconductive ring with one (AC-SQUID) or two (DC-SQUID) Josephson junctions.

Basic principles of the SQUID

The basic idea of the SQUID is that the phase of the wavefunction of the Cooper pairs is a *function* of the experimental parameters, i.e. it is *single-valued*. Since the domain of the phase function is topologically not trivial[2] and the same holds for the superconducting ring, it is possible that the phase always increases along the ring.

Let the ring initially be made by a bulk superconductor. Defining the *flux quantum* $\Phi_0 := h/2e$ and recalling equation (1.8) we can integrate the phase gradient over a closed loop in the ring, obtaining:

$$2n\pi = \oint \nabla\varphi \cdot \mathrm{dl} = \frac{2\pi}{\Phi_0}\left\{\oint \mathbf{A}\cdot\mathrm{dl} + \oint \frac{m}{2e^2\rho}\mathbf{J}\cdot\mathrm{dl}\right\}$$

[2]because of the identification $e^{i\varphi} = e^{i\varphi+i2n\pi}$ with $n \in \mathbb{Z}$.

whence it follows:

$$\Phi = n\Phi_0 \tag{3.1}$$

where $\Phi := \Phi_{geom} + Li$, Φ_{geom} is the geometric magnetic flux inside the loop, L is the ring inductance and i is the circulating supercurrent[3].

Now let the ring be interrupted by, say, two Josephson junctions[4]. Equation (3.1) becomes:

$$\Theta_1 - \Theta_2 = 2n\pi - 2\frac{\Phi}{\Phi_0}\pi$$

where we used the gauge invariant phase differences of the two junctions. This result is very important, since it links the magnetic flux inside the loop to the phases of the junctions and ultimately, via (2.17) and (2.21), to the total currents across them. Applying the RSJ model to the junctions and biasing the junctions with a current slightly greater than the critical supercurrent I_c, it is possible to show[9, 408] that the voltage response to small variations of the magnetic field is given by:

$$\delta V \approx \frac{R}{2L}\,\delta\Phi_{geom}$$

The sensitivity of this instrument is very low. Typical values are $R \sim 1\Omega$ and $L \sim 10^{-}9$ H, which give a final sensitivity of $\sim 1\mu V/\Phi_0$.

At present they still are, together with SERF magnetometers, the most sensitive technique to measure small magnetic fields[19].

Applications of the SQUID

The SQUID is an extremely versatile instrument. Firstly it has been used for long time to measure extremely small variations of magnetic fields, for instance in magnetotellurics[20].

Moreover, through magnetic coupling with an external circuit it can be used as an efficient low-signal galvanometer, voltmeter, ohmmeter (e.g. [21], [22]).

Thanks to their sensitivity and non-invasiveness, SQUIDs found many applications in medical diagnostics. SQUIDs have been used to monitorate brain activity as a complementary method to EEG (see e.g. [23]). They have found also application in cardiology, where MagnetoCardioGraphy (MCG) has the chance to accompany or perhaps substituting ECG. In basic research, they have achieved quite impressive results (see for instance [24]). On the contrary, in clinical environment, SQUID-MCGs are not so widely diffused[25].

Finally, SQUIDs have been successfully applied in the field of nondestrictive evaluation (NDE), for instance to study the almost dc corrosion

[3] We used Stokes' theorem to derive this result.

[4] In the following we analyse the DC-SQUID. At this level, the discussion of the AC-SQUID is very similar.

currents of materials. Their extremely high sensitivity over a wide range of frequencies makes them unparalleledly suitable instruments for this task[26].

3.1.2 Flux quantum and voltage standard

We have seen that a Josephson junction shows DC-energy steps, i.e. voltage steps, when an oscillating energy difference with the right frequency is superposed. In this sense a junction can be seen as a voltage-frequency converter. The conversion coefficient is Φ_0^{-1} (see (1.6) and (2.16)). Its most remarkable feature is that it depends only on universal constants. Since the environmental variables (magnetic field, junction dimensions, etc.) are not relevant, it can be measured in different places by different people. Moreover, it can be determined with a high degree of accuracy by means of frequency and voltage measurements.

Alternatively, by having a frequency standard and the value of Φ_0, one can establish a voltage standard. This is a significant progress, because frequencies can be measured and transmitted among different laboratories with relatively east-to-implement technologies. The main technique adopted before 1972 was that of Weston cells, which were difficult to transport. Their voltage output showed also a time drift. Hystorically, the discovery of Josephson junctions contributed to determine a readjustment of the fundamental constants in 1969[27]. More recently, single Josephson junctions have been replaced by arrays because of their higher accuracy, achieving in the last years a mutual agreement between national standard institutes better than 10^{-9}[28].

In the last years, arrays of Josephson junctions are also studied for "accurate and traceable measurement and generation of alternating (AC) voltage with arbitrary waveforms"[29].

3.1.3 Josephson computer technology

Well before 1962, scientists had already dreamed about logic circuitery based on superconductors. A first breakthrough in this field was the development of the *cryotron*[30], a device based on the superconductivity phase transition, controlled with magnetic field. The main problem of this approach was the relatively large time ($\sim 10\mu$s) needed to switch the device between the superconducting and the normal state. A solution was found soon after the publication of Josephson's article by Matisoo, in 1967. The key idea was the exploitation of the transition between zero-voltage and resistive states in a tunnel junction. The total current is always given by tunneling particles, respectively Cooper pairs and single electrons, and the junction dimensions are very small; the switching time is reduced by orders of magnitude. Matisoo also built up a pioneering Josephson digital circuit element, a flip-flop, that showed switching times smaller than 1 ns[31].

Matisoo worked for the leader corporation in computer technology at that time, i.e. International Business Machines Corporation (IBM). IBM was very interested in developing a possible Josephson digital system; Matisoo's article was in fact one of the first results of a research program on the topic, started in 1964. Josephson digital circuits show at least three main advantages:

1. very fast switching;
2. extremely low power dissipation;
3. very low temperatures, which allow use of superconducting strip lines, and reduce all temperature-dependent deterioration phenomena (corrosion, diffusion, electromigration);

IBM program culminated in 1980, when a dedicated issue of *IBM Journal of Research and Development* was devoted to this subject[32]. A review of the 1980 state-of-the-art physics and technology of Josephson logics is available in [33]. It is very interesting to quote some passages of the introductory report of Anacker[34], which are exemplifying of many other papers of that period:

> Josephson LSI[5] digital circuits have the potential for outperforming Si and GaAs semiconductor LSI circuits in both circuit speed and overall system performance. Such devices have in fact excellent potential for the realization of reliable computer mainframes with ultrahigh performance. [...]
>
> This range of processor cycle times, combined with current computer architecture, could provide mainframes with 10- to 100-fold higher computing rates than that of an IBM 3033 mainframe system. [...]
>
> If the hypothetical mainframe were implemented with semiconductor technology as used in the IBM 3033 system, it would dissipate (even with only 8M bytes of main memory) about 20 kW of power, an amount impossible to extract from such a small volume with today's cooling technology. [...] The hypothetical ultrahigh-performance mainframe[6] is, in contrast, estimated to dissipate less than 10 W when constructed with future Josephson circuit chips [...] This amount of heat could readily be extracted [...] by immersion of the packaged mainframe in a liquid helium bath. It appears, therefore, that Josephson technology may, at present, be *the only one* with potential for construction of mainframes of the ultrahigh performance defined previously.

[5] Large-Scale Integration.
[6] Based on Josephson junction technology.

Clearly, an enthusiastic mood permeated the considerations of Anacker and colleagues. However, nowadays superconducting computers are considered practically deprecated technology. The turning point of the scientific and economic trend is easy to identify with the help of the following graph, adapted from Hennessy and Jouppi[35].

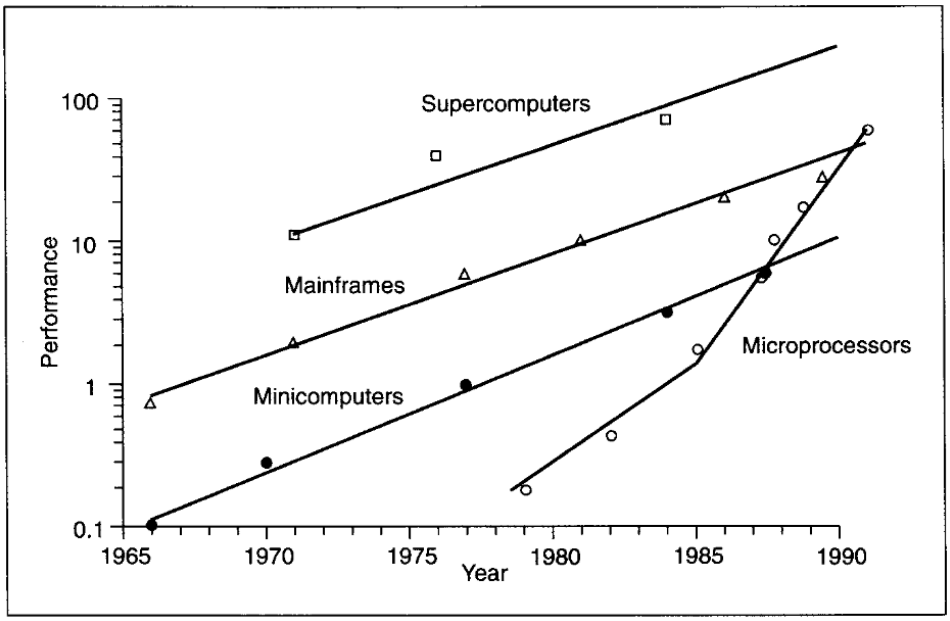

Figure 3.2: Performance against time for various types of computers. The exponential growth of the microprocessor performance is clear.

The killer technology of Josephson computer was the *microprocessor*. As many other exponential growths, Moore's law had been initially understimated; around 1985, the evolution of the microprocessor was so fast and well predictable that all concurrent technologies were practically abandoned. Until the first 90s, attempts were made to compare semiconductor- and superconductor-based computer technologies, and to hybridate them (see e.g. [36]). These attempts have failed so far, primarly because of market-economic reasons but also for intrinsic physical limits of Josephson technology. Excellent manufacturability and shorter design cycles of silicon chips makes them much more attractive, for a hypothehic investor, than superconducting chips, whose mass production feasibility has never been tested. Moreover, silicon technology has achieved extremely high levels of integration, that are probably impossible to obtain with Josephson technology, because of fundamental physical reasons:

> Information storage in Josephson memories is achieved by storing a flux quantum Φ_0 [...] in a superconducting loop. This requires [...] a minimum size to the storage loop. A number of practical and theoretical considerations conspire to impose a limit of the order 1 mA as the maximum critical current I_c of a Josephson device in such circuits. The inductance per unit lenght of the superconducting lines cannot be made much larger than about $5 \times 10^{-8} F/m$ for low impedance lines placed above a superconducting ground plane. Since $\Phi_0 \approx LI_c$ where L is the total loop inductance, this simple argument demands a loop area of the order of 1,000 square microns. Actually cell areas must be larger, to prevent interactions between cells and to accomodate address and sense lines[36, 2308].

For these reasons, large-scale production of superconducting computer has never started. Nowadays, silicon industry is dominating the market. Improvements in computer technologies are positively or negatively evaluated according to their compatibility with silicon technology. Integration with silicon is one of the key advantages of other technologies, like photonics.

Nevertheless, in the very last years Josephson circuits have regained interest, at least at the basic research stage, in the context of *qbit computers* (e.g. [37] and references therein).

3.2 Josephson-like effects

In the last years, enhancements in experimental techniques have allowed observation of Josephson-like effects in other quantum fluids than electrons. This is also theoretically very interesting, for it opens converging scenarios for superconductivity and other fields of basic research.

Equations (2.3) and (2.4) are very general. In our discussion, we attributed ψ to Cooper pairs. As a matter of fact, the whole theory could be used, say, for a Bose Einstein Condensate, provided that one is able to couple two BECs with a somehow insulating barrier. The advantages of this analogy are several. It provides a further confirmation of the general principles of quantum macroscopic effects (see section 1.3.3). Even more important, it could be exploited to prove theoretical predictions in difficult fields like Hi-T_c superconductivity, starting from the better-known theory of quasi-non-interacting atomic gases.

In the following, we discuss two kinds of systems that show quantum macroscopic effects, in particular Josephson-like effects: superfluid liquids, and trapped atomic gases.

3.2.1 Superfluid liquids

Superfluidity and superconductivity show many common features. For an extensive introduction to this topic, see [38]. Liquid superluidity is a phenomenon of low-temperature physics of liquids. Below a certain transition temperature, some liquid media show uncommon features. They can flow through very thin passages without any friction. Moreover, when one tries to make them rotate, they stay perfectly still. All properties of superfluids can be explained by assuming that some atoms condens into the same quantum ground state. This is basically the same behaviour of electrons in a superconductor, except for the neutrality of atoms. One thus expects superfluids to show coherent phenomena, as superconductors do, and among them the Josephson effect.

Superfluids can be divided in two classes, depending on the number of elementary particles composing every atom:

1. if it is even, atoms are complex[7] bosons. According to the theory of Bose-Einstein, they can directly gather into the ground state;

2. if this number is odd, atoms are complex fermions, and they form a bound ground state through pairing, exactly like electrons in superconductors.

The most studied liquid superfluid is helium, because it is the easiest to obtain in experiments. Helium can be found in two isopotes, ^{3}He and ^{4}He, the former being a complex fermion, the latter a complex boson. A characteristic shared by both isotopes of helium is electric neutrality. A voltage difference is not very effective on helium atoms, aside from multipole electromagnetical moments of neutral atoms. The driving force of the Josephson-like junction is, for neutral liquids, mechanical pressure. A superfluid junction is realized as follows. Some amount of liquid is pushed towards a wall with one or more small orifices. The orifices roughly behave for atoms like an insulating barrier does for electrons.

A first problem in the realization of a complete Josephson-like junction is that the wavefunction of a superfluid is coherent only for very short lenghts ($\sim$ nanometers), and it is very difficult to build so small holes. Moreover, atoms in a liquid present very complicated interactions, like many-body forces. A satisfactory theoretical picture is still lacking, and doing experiments without it is difficult. Experimental observations of Josephson-like effects in superfluids has been made, both for ^{3}He[39] and ^{4}He[40]. A superfluid analog of a DC-SQUID has been built recently by Packard *et al.*[41]. The theory of superfluid Josephson-like junctions has been reviewed by Thuneberg[42].

[7] We use the word "complex" to stress that atoms, similarly to Cooper pairs, are not elementary bosons. As a consequence, their behaviour at very high temperatures is different from that of, say, a photon, because they disintegrate.

3.2.2 Trapped atomic gases

The phenomenon of Bose Einstein Condensation (BEC) is the occupation of the ground state of a many-particle system by a macroscopically large number of particles. Its most studied realization, in the last years, has been in the field of atomic gases. The reason of this success is twofold. First of all, interactions among atoms in a neutral gas are weak, and their dynamics can be theoretically predicted through perturbative methods. Moreover, atomic gases can be spatially and energetically controlled by means of magnetic and optical traps. These allow experimental physicists to achieve extremely low temperatures, providing suitable conditions for observation of collective quantum phenomena (see section 1.3.3). The first successful realization of BEC in trapped atomic gases dates 1995[43].

A simple analogy can be established bewteen superconductors and atomic gases. In first approximation, an electric supercurrent is nothing but a free cloud of bosonic quasiparticles, i.e. the Cooper pairs. It behaves similarly to a gas of bosonic atoms in the ground state. There are two families of trapped atomic gases. The first is that of *Bose gases*, among which the most widely used is ^{87}Rb. Every single atom is formed by an even number of elementary particles of half-integer spin, therefore it is a complex boson. The second family is that of *Fermi gases* like ^{6}Li. The total number of elementary particles composing such an atom is odd, and the atom is a complex fermion. At very low temperature, fermionic atoms condens into pairs, exactly like elementary fermions. In fact, these pairs are also citied in the literature as "Cooper pairs". Bose gases are simpler to study than fermi gases, because the transition temperature for the BEC is significantly higher.

In fact, the theory of chapter 2 is not specific for superconductors and can be easily adapted to atomic gases (see e.g. eq. (2a) and (2b) in [44]). The main difference is that Cooper pairs in superconductors are electrically charged, while atomic gases are not. The mechanisms providing spatial and energetic confinements are different. The driving force of a gaseous Josephson-like junction is obviously not a voltage difference, but rather a chemical potential difference, originated through magnetic fields or laser detunings.

Bose gases

Two main experimental setup have been extensively studied: optical lattices and double-well potentials. In the first situation, atoms are trapped in a periodic potential. They are forced to stay on several equally spaced sites of a lattice, which is usually one-dimensional. Between two sites, an optical potential barrier plays the role of "insulator", analogously to the oxide layer in a normal SIS. Experimental observation of the a.c. Josephson effect in this geometry has been claimed by Inguscio *et al.* in 2001[45].

The double-well geometry has a basic advantage. It allows one to build a *single* Josephson junction, rather than an array. Modularity is usually a key component in technologic progress. For instance, realization of two single junctions is a necessary condition for an atomic equivalent of the SQUID. In 2005 Oberthaler *et al.* reported the first successful realization of the Josephson effect in a double-well potential[46]. Figure 3.2.2 is taken from the same article; oscillations of the gas between the two wells are clearly visible. More recently, Steinhauer *et al.* pointed out that alternating currents seen in [46] are not a direct observation of the a.c. Josephson effect, but rather a correlated phenomenum called *plasma oscillations*. Briefly explained, the phase difference between the condensates in the two wells is not a monotone function of time, as in the a.c. Josephson effect at constant voltage difference, but rather oscillates around its equilibrium value. The authors also claimed to have succeded in the first realization of a single bosonic Josephson junction, and in the first observation of a.c. and d.c. Josephson effect in bose gases[47]. This result is reported in figure 3.2.2, which has to be interpreted as follows. The vertical axes represents the population imbalance between the wells:

$$\eta := \frac{1}{2}\left(\rho_{\mathbf{L}} - \rho_{\mathbf{R}}\right)$$

Its derivative $\dot{\eta}$ is the non-electric analog the the Josephson current density of equation (2.12). As a matter of fact, we could choose the same variable in our discussion, for it holds:

$$\frac{\partial \rho_{\mathbf{L}}}{\partial t} = -\frac{\partial \rho_{\mathbf{R}}}{\partial t} \quad \Longrightarrow \quad J := 2e\frac{\partial \rho_{\mathbf{L}}}{\partial t} = 2e\dot{\eta}$$

Assuming approsimation (2.11), this current is a sinus. Neglecting all other current density components because of the experimental setup of [47], its primitive function has to be a cosinus, which is basically the curve observed in figure 3.2.2.

At the present state of research, physicists are trying to realize a gaseous version of the SQUID. Experimentally, this is a very demanding task, because of the complex trap geometry. It is necessary to merge one or two double well potentials into a ring-shaped trap, respectively for the AC and DC SQUID.

Fermi gases

A similar topic of intense research is Josephson-like effects in cold atomic Fermi gases. The state-of-the-art experiments have not succeded yet in observing directly a Josephson-like effect. Theoretical studies have been published by several authors (e.g.[48][49]). Practical methods to achieve

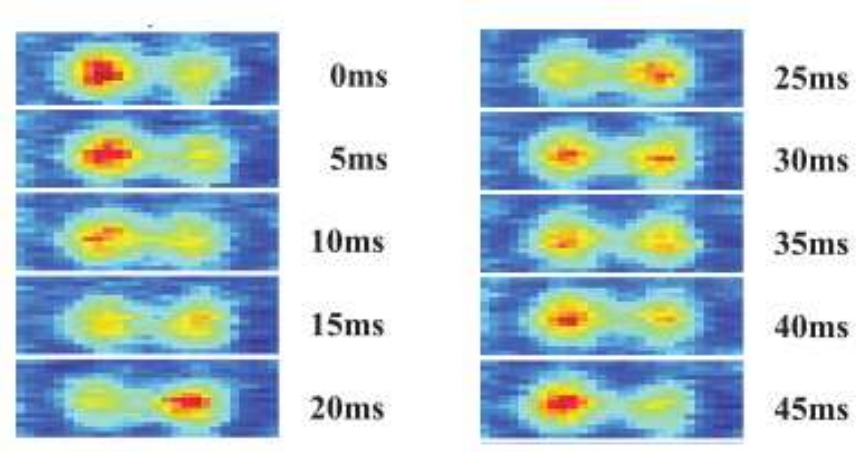

Figure 3.3: Josephson oscillations in an atomic bose gas. The experimental setup is the double well potential. Data adapted from Oberthaler *et al.*[46].

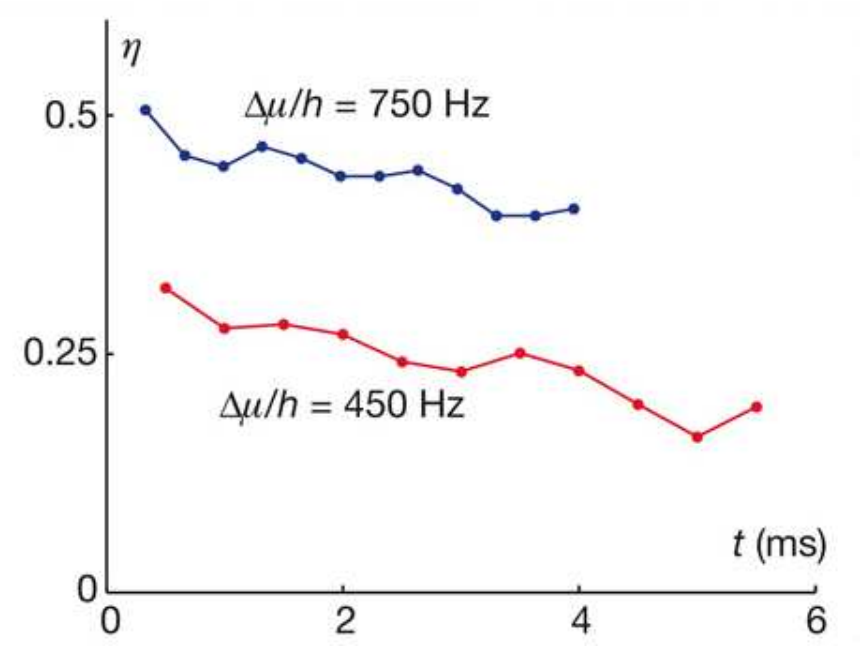

Figure 3.4: Population imbalance η vs time in a double-well potential trap, for a gas of ^{87}Rb. As discussed above in the text, the AC Josephson effect is the small modulation of $\eta(t) \propto \cos(\omega_{\Delta\mu/\hbar} t)$. Their frequencies are determined by the chemical potential difference $\Delta\mu$. According to the authors, the slope of the curves is due to imaging losses. Data adapted from Steinhauer *et al.*[47].

Josephson oscillations have also been developed[50]. In the last year, numerical methods to simulate Josephson oscillations have been studied[51].

Summary

This work aims to be a simple, yet extensive introduction to the Josephson effect. The origins of the effect were investigated at the beginning, and the problem of phase decoherence was explicitely addressed. It was shown that superconductivity is a coherent macroscopic phenomenon. Then the two-state theory of the Josephson effect was presented. The simplest model of a Josephson junction was introduced, and its predictions were verified by our experimental data. The most relevant applications of the Josephson effect were discussed, among them computer technology based on Josephson junctions. Finally, the generality of the Josephson theory could be appreciated. Analog effects in superfluids and cold atomic gases were reviewed, and recent experimental data, which confirm the theoretical predictions, were shown.

Bibliography

[1] R. P. Feynman. *Feynman lectures on physics. Volume 3: Quantum mechanics*. Reading, Ma.: Addison-Wesley, 1965, edited by Feynman, Richard P.; Leighton, Robert B.; Sands, Matthew, 1965.

[2] B.D. Josephson. Possible new effects in superconductive tunnelling. *Physics Letters*, 1:251–253, July 1962.

[3] V. Moretti. Struttura matematica delle teorie quantistiche e teoria spettrale in spazi di hilbert, http://www.science.unitn.it/~moretti/dispense.html, 2007.

[4] L.D. Landau and E.M. Lifshitz. *Statistical Physics*. Butterworth-Heinemann, 1980.

[5] K. Huang. *Statistical mechanics*. New York: Wiley, —c1987, 2nd ed., 1987.

[6] K.H. Bennemann and John Boyd Ketterson. *The Physics of Superconductors: Conventional and High-Tc Superconductors*. Springer, 2003.

[7] J. Bardeen, L. N. Cooper, and J. R. Schrieffer. Theory of superconductivity. *Phys. Rev.*, 108(5):1175–1204, Dec 1957.

[8] V. L. Ginzburg and L.D. Landau. On the theory of superconductivity. *Zh. Eksperim. i Teor. Fiz*, 1950.

[9] Antonio Barone and Gianfranco Paternò. *Physics and applications of the Josephson effect*. John Wiley and Sons, 1982.

[10] Sidney Shapiro. Josephson currents in superconducting tunneling: The effect of microwaves and other observations. *Phys. Rev. Lett.*, 11(2):80–82, Jul 1963.

[11] L. de Broglie. Ondes et quanta. *C. R. Acad. Sc.*, 177:507, 1923.

[12] K.K. Likharev. *Dynamics of Josephson junctions and circuits*. Gordon and Breach Science Publishers, 1986.

[13] D. E. McCumber. Effect of ac impedance on dc voltage-current characteristics of superconductor weak-link junctions. *Journal of Applied Physics*, 39(7):3113–3118, 1968.

[14] W. C. Stewart. Current-voltage characteristics of josephson junctions. *Applied Physics Letters*, 12(8):277–280, 1968.

[15] W. C. Scott. Hysteresis in the dc switching characteristics of josephson junctions. *Applied Physics Letters*, 17(4):166–169, 1970.

[16] J. G. Bednorz and K. A. Müller. Possible high t_c superconductivity in the balacuo system. *Zeitschrift für Physik B Condensed Matter*, 64(2):189–193, June 1986.

[17] V. V. Ryazanov, V. A. Oboznov, A. Yu. Rusanov, A. V. Veretennikov, A. A. Golubov, and J. Aarts. Coupling of two superconductors through a ferromagnet: Evidence for a π junction. *Phys. Rev. Lett.*, 86(11):2427–2430, Mar 2001.

[18] Antonio Barone. The strong impact of the weak superconductivity. *Journal of Superconductivity*, 17(5):585–592, October 2004.

[19] D. Budker and M. V. Romalis. Optical magnetometry, 2006.

[20] T. D. Gamble, W. M. Goubau, and J. Clarke. Magnetotellurics with a remote magnetic reference. *Geophysics*, 44(1):53–68, 1979.

[21] E. Il'ichev, L. Dorrer, F. Schmidl, V. Zakosarenko, P. Seidel, and G. Hildebrandt. Current resolution, noise, and inductance measurements on high-t_c dc squid galvanometers. *Applied Physics Letters*, 68(5):708–710, 1996.

[22] A. H. Miklich, D. Koelle, F. Ludwig, D. T. Nemeth, E. Dantsker, and John Clarke. Picovoltmeter based on a high transition temperature squid. *Applied Physics Letters*, 66(2):230–232, 1995.

[23] A I Ahonen, M S Hämäläinen, M J Kajola, J E T Knuutila, P P Laine, O V Lounasmaa, L T Parkkonen, J T Simola, and C D Tesche. 122-channel squid instrument for investigating the magnetic signals from the human brain. *Physica Scripta*, T49A:198–205, 1993.

[24] J. Kawai, M. Kawabata, T. Shimozu, M. Miyamoto, Y. Adachi, G. Uehara, K. Komamura, and N. Tsuyuguchi. A low noise squid magnetometer array probe designed for mouse and rat mcg measurements. *International Congress Series*, 1300:570–573, 2007.

[25] H. Koch. Squid magnetocardiography: status and perspectives. *Applied Superconductivity, IEEE Transactions on*, 11(1):49–59, Mar 2001.

[26] W G Jenks, S S H Sadeghi, and J P Wikswo Jr. Squids for nondestructive evaluation. *Journal of Physics D: Applied Physics*, 30(3):293–323, 1997.

[27] W. H. Parker, B. N. Taylor, and D. N. Langenberg. Measurement of 2e/h using the ac josephson effect and its implications for quantum electrodynamics. *Phys. Rev. Lett.*, 18(8):287–291, Feb 1967.

[28] Clark A. Hamilton. Josephson voltage standards. *Review of Scientific Instruments*, 71(10):3611–3623, 2000.

[29] O.A. Chevtchenko, H.E. van den Brom, E. Houtzager, R. Behr, J. Kohlmann, J.M. Williams, T.J.B.M. Janssen, L. Palafox, D.A. Humphreys, F. Piquemal, S. Djordjevic, O. Monnoye, A. Poletaeff, R. Lapuh, K.-E. Rydler, and G. Eklund. Realization of a quantum standard for ac voltage: overview of a european research project. *Instrumentation and Measurement, IEEE Transactions on*, 54(1):628– 631, Apr 2005.

[30] D.A Buck. The cryotron-a superconductive computer component. *Proceedings of the IRE*, 42(4):482–493, Apr. 1956.

[31] J. Matisoo. The tunneling cryotron—a superconductive logic element based on electron tunneling. *Proceedings of the IEEE*, 55(2):172–180, Feb. 1967.

[32] Ibm journal of research and development. Technical report, IBM, 1980.

[33] J.Matisoo. Overview of josephson technology logic and memories. *IBM Journal of Research and Development*, 24:113–129, 1980.

[34] W. Anacker. Josephson computer technology: An ibm research project. *IBM Journal of Research and Development*, 24:107–112, 1980.

[35] John L. Hennessy and Norman P. Jouppi. Computer technology and architecture: An evolving interaction. *Computer*, 24(9):18–29, 1991.

[36] H. Kroger and U. Ghoshal. Can superconductive digital systems compete with semiconductor systems? *Applied Superconductivity, IEEE Transactions on*, 3(1):2307–2314, Mar 1993.

[37] Yuriy Makhlin, Gerd Schön, and Alexander Shnirman. Quantum-state engineering with josephson-junction devices. *Rev. Mod. Phys.*, 73(2):357–400, May 2001.

[38] D.R. Tilley and J. Tilley. *Superfluidity and Superconductivity.* CRC Press, 1990.

[39] S. V. Pereverzev, A. Loshak, S. Backhaus, J. C. Davis, and R. E. Packard. Quantum oscillations between two weakly coupled reservoirs of superfluid 3he. *Nature*, 388:449–451, Jul 1997.

[40] Kalyani Sukhatme, Yury Mukharsky, Talso Chui, and David Pearson. Observation of the ideal josephson effect in superfluid 4he. *Nature*, 411:280–283, May 2001.

[41] Emile Hoskinson, Yuki Sato, and Richard Packard. Superfluid [sup 4]he interferometer operating near 2 k. *Physical Review B (Condensed Matter and Materials Physics)*, 74(10):100509, 2006.

[42] Erkki Thuneberg. Theory of josephson phenomena in superfluid 3he. *AIP CONFERENCE PROCEEDINGS*, 850:103, 2006.

[43] M. H. Anderson, J. R. Ensher, M. R. Matthews, C. E. Wieman, and E. A. Cornell. Observation of Bose-Einstein Condensation in a Dilute Atomic Vapor. *Science*, 269(5221):198–201, 1995.

[44] A. Smerzi, S. Fantoni, S. Giovanazzi, and S. R. Shenoy. Quantum coherent atomic tunneling between two trapped bose-einstein condensates. *Phys. Rev. Lett.*, 79(25):4950–4953, Dec 1997.

[45] F. S. Cataliotti, S. Burger, C. Fort, P. Maddaloni, F. Minardi, A. Trombettoni, A. Smerzi, and M. Inguscio. Josephson Junction Arrays with Bose-Einstein Condensates. *Science*, 293(5531):843–846, 2001.

[46] Michael Albiez, Rudolf Gati, Jonas Folling, Stefan Hunsmann, Matteo Cristiani, and Markus K. Oberthaler. Direct observation of tunneling and nonlinear self-trapping in a single bosonic josephson junction. *Physical Review Letters*, 95(1):010402, 2005.

[47] J. Steinhauer, S. Levy, E. Lahoud, and I. Shomroni. The a.c. and d.c. Josephson effects in a Bose-Einstein condensate. *APS Meeting Abstracts*, pages 4006P–+, May 2008.

[48] M. Wouters, J. Tempere, and J. T. Devreese. Path integral formulation of the tunneling dynamics of a superfluid fermi gas in an optical potential. *Phys. Rev. A*, 70(1):013616, Jul 2004.

[49] L. Pezzè, L. Pitaevskii, A. Smerzi, S. Stringari, G. Modugno, E. de Mirandes, F. Ferlaino, H. Ott, G. Roati, and M. Inguscio. Insulating behavior of a trapped ideal fermi gas. *Phys. Rev. Lett.*, 93(12):120401, Sep 2004.

[50] Gh.-S. Paraoanu, M. Rodriguez, and P. Törmä. Josephson effect in superfluid atomic fermi gases. *Phys. Rev. A*, 66(4):041603, Oct 2002.

[51] S. K. Adhikari. Josephson oscillation of a superfluid fermi gas. *The European Physical Journal D - Atomic, Molecular, Optical and Plasma Physics*, 47(3):413–419, May 2008.